Journal of
Composites Science

MDPI

Article

Antimicrobial Hydrophobic SiO_2-TiO_2-PDMS Films: Effect of Indirect Ultrasonic Irradiation on the Synthesis Process

Alicia Rosales [1,2], Hugo Mandujano [1], José Antonio Cervantes-Chávez [3] and Karen Esquivel [1,*]

[1] Graduate and Research Division, Engineering Faculty, Universidad Autónoma de Querétaro, Cerro de las Campanas, Santiago de Querétaro 76010, Mexico; alicia.ros.perez@hotmail.com (A.R.); hugo.almg99@hotmail.com (H.M.)
[2] Centro de Investigación en Química para la Economía Circular, CIQEC, Facultad de Química, Universidad Autónoma de Querétaro, Cerro de las Campanas, Santiago de Querétaro 76010, Mexico
[3] Natural Sciences Faculty, Universidad Autónoma de Querétaro, Carr. Chichimequillas-Anillo Vial Fray Junípero Serra, Km 8, Santiago de Querétaro 76000, Mexico; cervanteschavez@gmail.com
* Correspondence: karen.esquivel@uaq.mx; Tel.: +52-442-192-1200 (ext. 65401)

Abstract: Film applications' recent advances in the alimentary industry mainly focus on extending product shelf life. Researchers have investigated the use of nanomaterials as active packaging to shield food product contents from the outside elements and prevent bacterial development. In this context, the use of sonochemistry energy offers a friendly and efficient opportunity to obtain this kind of film. However, access to an ultrasonic homogenizer is limited because of the cost and accessories. In this work, a self-cleaning coating based on the SiO_2-TiO_2-PDMS composite was obtained by the sol–gel method coupled with indirect sonochemical energy. Two sonication reaction times were used to investigate its impact on the final composite's chemical, morphological, and antibacterial properties. TEM and SEM techniques indicate an amorphous morphology and superficial cracks in SiO_2-TiO_2-PDMS films over aluminum foil. At the same time, AFM reveals a rise in rugosity with a value of Ra = 18.7 ± 2.47 nm, increasing the sonochemical reaction time. Non-significative changes by FTIR-ATR analysis were observed. The antibacterial evaluation was conducted, and the results indicate that both composites exhibited superior effectiveness. Specifically, the S40 film demonstrated a significant reduction in the growth of Gram-negative cells (*E. coli*, *P. putida*, and *P. aeruginosa*), with reductions ranging from 50% to 95%. In contrast, the reduction in Gram-positive cells (*S. aureus*) was less than 10%. These findings underscore the potential application of the SiO_2-TiO_2-PDMS film as active packaging.

Keywords: antimicrobial activity; ultrasonic irradiation; hydrophobicity; active package; SiO_2-TiO_2

check for updates

Citation: Rosales, A.; Mandujano, H.; Cervantes-Chávez, J.A.; Esquivel, K. Antimicrobial Hydrophobic SiO_2-TiO_2-PDMS Films: Effect of Indirect Ultrasonic Irradiation on the Synthesis Process. *J. Compos. Sci.* **2024**, *8*, 104. https://doi.org/10.3390/jcs8030104

Academic Editor: Francesco Tornabene

Received: 29 January 2024
Revised: 21 February 2024
Accepted: 12 March 2024
Published: 16 March 2024

1. Introduction

Packaging materials protect and insulate the food products from exterior conditions and guarantee safety. The alimentary industry exhibits high economic costs for damage and loss of products, mainly for transportation and shelf life. The packages act as a physical barrier, reducing foods' postharvest and production losses and preserving their quality, flavor, and freshness [1]. Films and coatings with multi-properties have been developed with significant interest for material protection from chemical, physical, mechanical, and microbial damage. The multi-properties films involve the development of surfaces such as self-cleaning, corrosion-resistant, oil-repellent, antibacterial, antifouling, and mechanical resistance [2].

Recently, there has been growing attention to technological innovations in alternative materials for packaging, which can prolong the shelf-life and preserve the food's quality. This packaging system is called active packaging. Different parameters are considered for food quality control, including water activity, pH, temperature, oxygen content, and

presence or absence of light. Consequently, the food packaging is designed based on these parameters [3].

Active packaging incorporates active agents into a polymeric matrix, producing flexible active films with mono- or multilayer structures [4]. Another approach to improving functional packaging films is using polymers [5], such as polydimethylsiloxane (PDMS), to functionalize the film by manipulating the hydrophobic properties and improving the film's mechanical properties (Table S1) [6–8]. On the other hand, nanomaterials (NMs) have been considered a good option for coatings over conventional package materials (cardboard, aluminum, and plastic) [9–11]. Specifically, for active antimicrobial packaging, Ag, $AgNO_3$, ZnO, TiO_2, and MgO nanoparticles (NPs) have been studied (Table S1) [11–14]. The action mechanisms of these NPs are described as direct interactions with microbial cells and electron transference in the transmembrane, penetration of the cell, cellular components oxidation, and reactive oxygen species (ROS) generation [9].

The film's deposition to create a feasible film for active packaging involves temperature control to improve the adherence with the surface without advising the surface's nature (roughness or smoothness) [15–17]. An option to overcome the film's adherence is to obtain nanosized materials (NMs) through an effective, efficient, and environmentally friendly technique such as the sonochemical method, which offers greater selectivity, reactivity, and yields, a decrease in reaction time and, less toxic residues [18].

In this context, through ultrasonic cavitation in the solution by forming micro-bubbles, which grow and collapse, imploding and generating hot spots (5000 K and 1000 atm) [19], it is possible to promote the chemical reactions, forming oxidative species, an ideal chemical environment for NMs synthesis. The ultrasound irradiation could be applied in two direct and indirect methods; the direct method uses horn systems for high intensity, and the indirect method employs bath for low power [20,21]. Schneider et al. (2020) analyzed the impact of the ultrasonication method on metal oxide particle synthesis, and the sonication method modified the particles dispersion [22]. The election of the way of ultrasound irradiation depends on the frequency, amount of power, volume, and uniform distribution cavitation activity [23]. The indirect method in the ultrasonic bath is used for a specific power or ultrasonic intensity because it is not possible to change it for this type of sonochemical reactor; that is why it is needed to control external variables of the synthesis process to obtain uniform and high efficiency from ultrasonic irradiation [20].

It is essential to establish that the election of the sonochemical method depends on the equipment's availability, access, and cost, which will affect the final decision of the synthesis method and NMs application.

Previous research on SiO_2-TiO_2 coatings synthesized by the sol–gel method coupled to direct ultrasonic irradiation showed that using different conditions of sonochemistry, such as amplitude and cavitation, affected the final morphology, physic (hydrophobicity, softness, roughness, mechanical resistance, and morphological form) and chemical (photocatalytic and hydrophobic) properties [24]. Taking this background as a starting point, in the present work, the SiO_2-TiO_2 composite was synthesized by the sol–gel method coupled to ultrasonic irradiation in an indirect method, which is considered a novel and practical synthesis method to obtain a SiO_2-TiO_2 film for outer packaging.

2. Materials and Methods

2.1. Materials and Bacteria Species

For the preparation of the SiO_2-TiO_2 films, the following precursors and reagents were used: titanium isopropoxide (TTIP, 97%, Sigma Aldrich, Toluca, Mexico), tetraethyl orthosilicate (TEOS, 98%, Sigma Aldrich, Toluca, Mexico), absolute ethyl alcohol (EtOH, 98%, JT Baker, CDMx, Mexico), polydimethylsiloxane (PDMS, Sigma Aldrich, Toluca, Mexico), oxalic acid dihydrate (AcOx, JT Baker, CDMx, Mexico), distilled water (H_2O). The SiO_2-TiO_2 composite was synthesized by modifying the sol–gel method previously reported [25]. The molar ratio of TEOS, EtOH, H_2O, PDMS, TTIP, and AcOx was 1:5.5:5.6:0.05:0.15:0.05.

The synthesis was conducted using an ultrasonic bath (Branson 1510 Ultrasonic Cleaner, MS Ultraschall Technologie GmbH, Lansing, MI, USA) with 40 kHz energy.

Log-phase cultures of *Escherichia coli* (Top10, Gram-negative), *Staphylococcus aureus*, Gram-positive), *Pseudomonas aeruginosa ATCC* 9072 (Gram-negative), and *Pseudomonas aeruginosa* (Gram-negative; clinical isolate resistant to levofloxacin (LEV)) were used for the analysis of the antimicrobial assay. These strains were recovered from −80 °C on LB agar plates (MCB LAB) at 37 °C for 24 h.

2.2. SiO_2-TiO_2 Synthesis and Characterizations

The synthesis of the SiO_2-TiO_2 films was conducted by modifying the procedure proposed by Rosales et al. (2018) [25] using an indirect ultrasonic source. The sol of SiO_2 was formed with a solution of EtOH, AcOx, and H_2O and irradiated with ultrasonic energy for 15 min. After TEOS was added dropwise, the mixture continued to be irradiated with ultrasonic energy for 3 min. Later, PDMS was added dropwise under continuous ultrasonic energy for another 3 min. The TiO_2 sol was prepared by adding TTIP dropwise to isopropyl alcohol under a nitrogen atmosphere and constant magnetic stirring. The TiO_2 and the SiO_2 sols were mixed, and immediately after mixing, 10 mL of distilled water was added at the ultrasonics conditions over 30 min and 40 min, obtaining two composites, SiO_2-TiO_2-S30 and SiO_2-TiO_2-S40, respectively. Reaction times were determined based on sonochemical reaction times previously studied by Rosales et al. (2021) [24]. Once the composites were obtained, they were applied over 1 × 4 cm aluminum foil using the painting method [26] to form a uniform film; in the case of glass, 2 × 7 cm glass slides were used, employing the imprint method. SiO_2-TiO_2 composites were deposited over a glass substrate to evaluate their physical–chemical properties and over an aluminum foil substrate to evaluate their antimicrobial activity.

The SiO_2-TiO_2 composites as powder were observed by electronic transmission microscopy (TEM) using a JOEL JEM-1010 operating at 200 kV, and the particle size was measured with Image J® software version 1.54i. The FTIR spectra were realized in a range of 4000 to 650 cm^{-1} using an IRAffinity-1S equipped with an ATR instrument. The SiO_2-TiO_2 films applied over the aluminum foil were examined by scanning electron microscopy (SEM) using a JOEL JSM-6060 LV (Tokio, Japan), operating at 15 kV. The crystallinity of the SiO_2-TiO_2 films over a glass substrate was determined by X-ray diffraction (XRD) with angles of $10 < 2\theta < 80°$ in a pitch of 0.01 using an X-ray diffractometer (D8, Bruker) with a Cu target and Ni filter ($\lambda_{CuK\alpha}$ = 1.54 Å).

SiO_2-TiO_2 films applied over a glass substrate were analyzed by atomic force microscopy (AFM) employing a Bruker Dimension edge with Scan Assyst to obtain rugosity information. The contact angle of the SiO_2-TiO_2 films over the glass was determined by employing distilled water droplets using the manual drop shape with the ImageJ® software. Water droplets of 10 µL were placed at three different positions on the surface, and the average value was reported as the contact angle (θ). The thickness of the SiO_2-TiO_2 films applied onto glass were analyzed using optical analysis of profilometry employing a Dektak 6M Stylus Profilerc with a diamond tip of 6 µm and a force of 8 mg, assisted by a digital microscope VH 2500R Keyence (Mechelen, Belgium).

2.3. Films Antimicrobial Activity Evaluation

The antimicrobial activity was evaluated against *Escherichia coli*, *Staphylococcus aureus*, *Pseudomonas aeruginosa* levofloxacin (LVX) resistant, and *Pseudomonas aeruginosa* (ATCC 9027) by measuring the survival percentage of bacteria using aluminum foil coated with SiO_2-TiO_2-S30 and S40 films.

Bacterial cell cultures were prepared for each strain as follows: 5 colonies were taken to be inoculated in 5 mL of Luria–Bertani (LB) medium in a 50 mL sterile conic tube. The tubes were incubated at 37 °C (for 5 h), shaking at 150 rpm until the optical density measured at 600 nm (OD_{600nm}) of the cultures reached 0.1 (1×10^6 CFU (colony forming units)/mL)). Then, aluminum foil, SiO_2-TiO_2-S30 and -S40 films over aluminum foil with 1 × 4 cm

dimensions were (previously autoclaved) placed inside the corresponding culture. The incubation was carried out for 4 h under above mentioned conditions, exposed to visible light to determine the bactericidal activity. Pristine aluminum foil was used as a negative control.

After interactions between the foil and bacterial cell cultures, 100 µL aliquot of each culture was spread using sterile glass beads onto duplicate fresh LB agar medium plates and incubated at 37 °C for 24 h. All interactions were carried out the same way for the different bacterial strains. The number of CFU was scored, and the percentage reduction in cell viability was calculated based on the CFU count obtained from the control plate (pristine aluminum foil). The experiments were conducted in triplicate.

3. Results and Discussion

3.1. Composite and Film Characterization

TEM and SEM analyses were carried out to observe the morphology of the SiO_2-TiO_2 composites. The TEM analysis was carried out with the composite as powder. For the SEM analysis, the composite was observed as a film over aluminum foil. The transmission and scanning micrographs are shown in Figure 1.

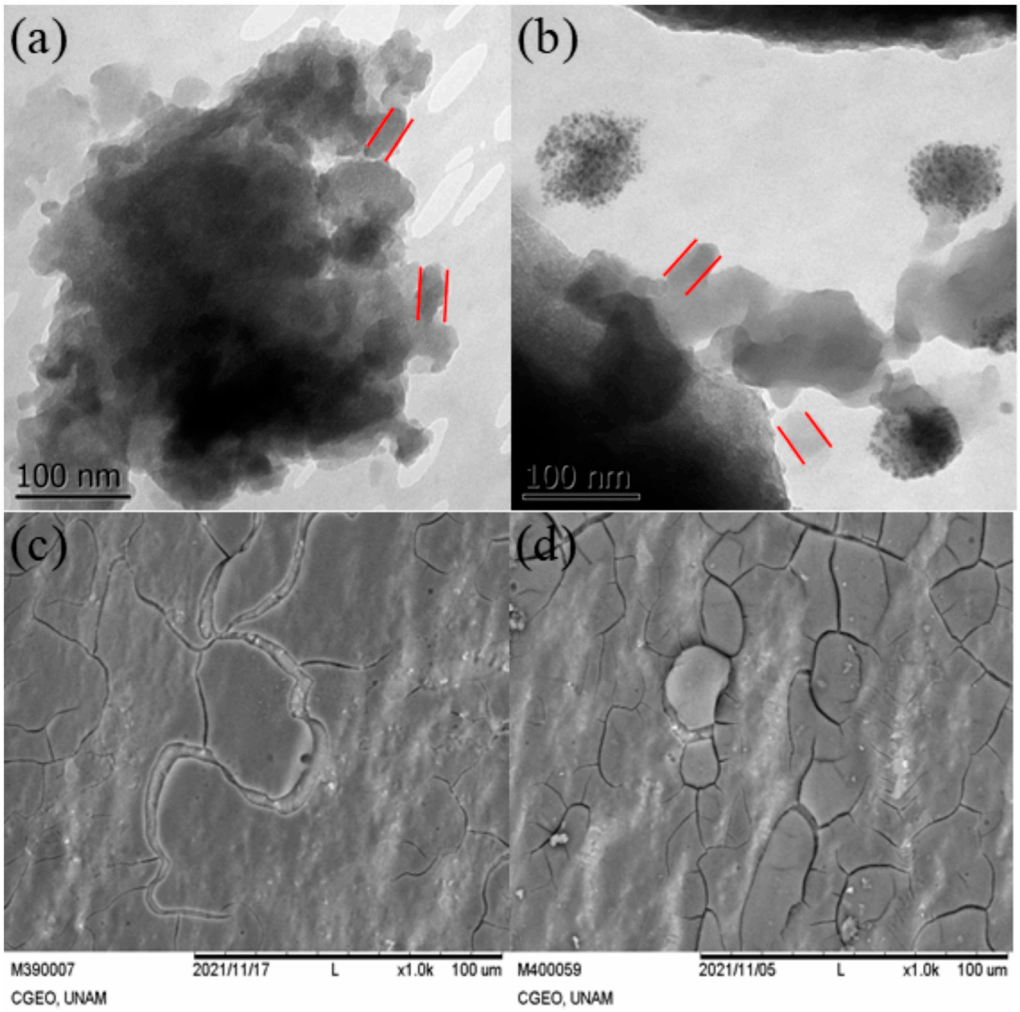

Figure 1. TEM images of SiO_2-TiO_2 composite (**a**) S30, (**b**) S40, and SEM images of SiO_2-TiO_2 films (**c**) S30, and (**d**) S40. The red lines mark the average size.

TEM images of the SiO_2-TiO_2-S30 and -S40 (Figure 1a,b) exhibit irregular morphology and sheets forming layers. In Figure 1a, it is possible to observe for the SiO_2-TiO_2-S30 sample an agglomerate with small particles, measured with ImageJ®, having an average of

30 nm particle diameter (red lines), and the cluster average size was 350 nm. The particles are agglomerated with some dark points on the edge. On the other hand, the SiO_2-TiO_2-S40 sample (Figure 1b) also shows an irregular morphology with layers, with an average size of 60–130 nm (red lines), and with some dark points clusters with an average size of 1–3 nm, which corresponds to the TiO_2. In this way, Kapridaki et al. (2018) observed in SiO_2-TiO_2-PDMS composites TEM images synthesized by sol–gel without sonochemistry, a network of aggregates, and connectivity of Ti-O-Si at an atomic level. Furthermore, increasing the addition of oxalic acid improved the detection of TiO_2 particles [27,28]. In our case, using ultrasonic energy and the increased reaction time allowed for similar results in the SiO_2-TiO_2-S40 film to be obtained [29]. Furthermore, indirect ultrasonic irradiation decreases the TiO_2 NPs dispersion compared to the direct method. Nevertheless, it was demonstrated that the formation of clusters depends on the reaction time [30]

SEM images of the SiO_2-TiO_2 films (Figure 1c,d) at 500× (inset) and 1000× present micro-fissures. The SiO_2-TiO_2-S40 sample shows fewer cracks and some pores over the surface. Meanwhile, the SiO_2-TiO_2-S30 displays more cracks and slices over the surface. In 1000×, the cracks are more noticeable; these results have been previously reported over steel substrates [31], which demonstrated that the application of the method of sonochemistry produces similar morphologies.

The three-dimensional AFM of the SiO_2-TiO_2 films on a glass substrate in an area of 10 × 10 μm is shown in Figure 2. The formation of craters and elevations are visible along the topographic surface, which is attributed to the TiO_2 nanoparticles [32]. Similar results were found by Widati et al. (2019) using 0.015 and 0.030 molar of TiO_2 exhibiting low NPs homogeneity over the surface [33]. These formations are more pronounced in the SiO_2-TiO_2-S40 film (Figure 2b), where the low concentration of NPs prevents their random distribution on the surface. The roughness value for the S30 and S40 films was Ra = 11.55 ± 1.33 nm and Ra = 18.7 ± 2.47 nm, respectively. Showing that if the ultrasonic reaction time increases from 30 to 40 min, an increment of roughness is also detected. In this way, Sebastian et al. (2018) evaluated PDMS/SiO_2 films over an aluminum surface with different concentrations of functional SiO_2, synthesized in an ultrasonic system showing no change in the films' roughness [34]. The morphological changes depend on the ultrasonic energy application method utilized during the synthesis process in this study. In this context, the thickness of the SiO_2-TiO_2 films was previously determined, obtaining a range between 650 and 700 μm.

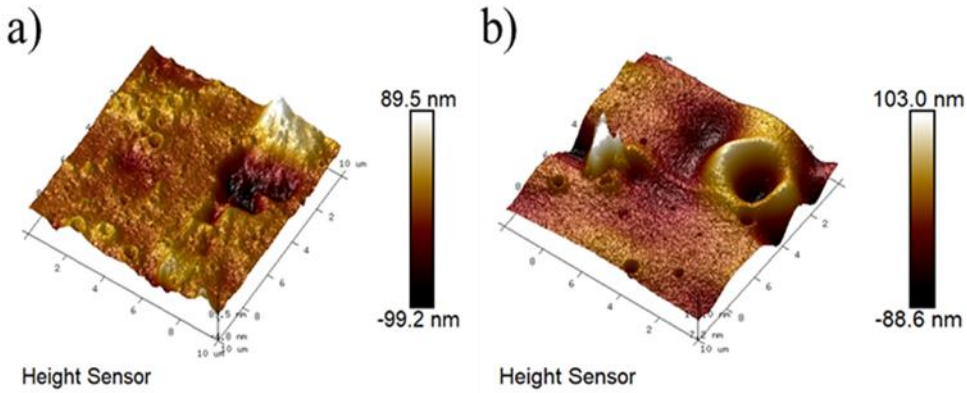

Figure 2. AFM micrographs of the SiO_2-TiO_2 (**a**) 30 (**b**) 40 films.

The SiO_2-TiO_2 composites were analyzed by ATR-FTIR from 4000 to 650 cm^{-1}, as shown in Figure 3. A band at 2964 cm^{-1} is observed, which is assigned to the asymmetric stretching vibration of C-H bonds in CH_3 groups [35], and this band is more intense in the S30 composite. The band at 839 cm^{-1} corresponds to the Si-OH group. The bands at 850 and 800 cm^{-1} (Si-O stretching mode) were assigned to the CH_3 rocking of PDMS and TEOS [36]. These last bands correspond to the asymmetric and symmetric stretching and bending vibration of Si-O-Si. The bands at 903 and 1261 cm^{-1} correspond to the Si-C

stretching vibrations and the Si-CH_3 group symmetric deformation of PDMS of -CH_3 in Si-CH_3 [36,37]. The band at 1423 cm^{-1} is attributed to asymmetric C-H bending on Si-CH_3, and 2157 cm^{-1} corresponds to Si-H stretching [38]. The band at 1680 cm^{-1} corresponds to vibrations of oxalic acid. The signal at 1687 cm^{-1} is attributed to vibrations of the Si-O-bonds in TEOS/PDMS. This signal is more intense and shifts to the left in the S40 sample, indicating a formation of the silanol group (Si-OH) [39]. The signals over the band at 1000 at 1200 cm^{-1} summarize the vibrations at 1062 and 1092 cm^{-1} of the Si-O-Si (stretching) [40]. The band observed at 700 cm^{-1} is attributed to the rocking vibration of $-(CH_2)_n$ of the residual ethanol in the films [41]. The bands at 1500 to 1300 cm^{-1} are attributed to the C-H stretching and bending modes of the residual organic groups in the film [42], which are more visible in the S40 composite.

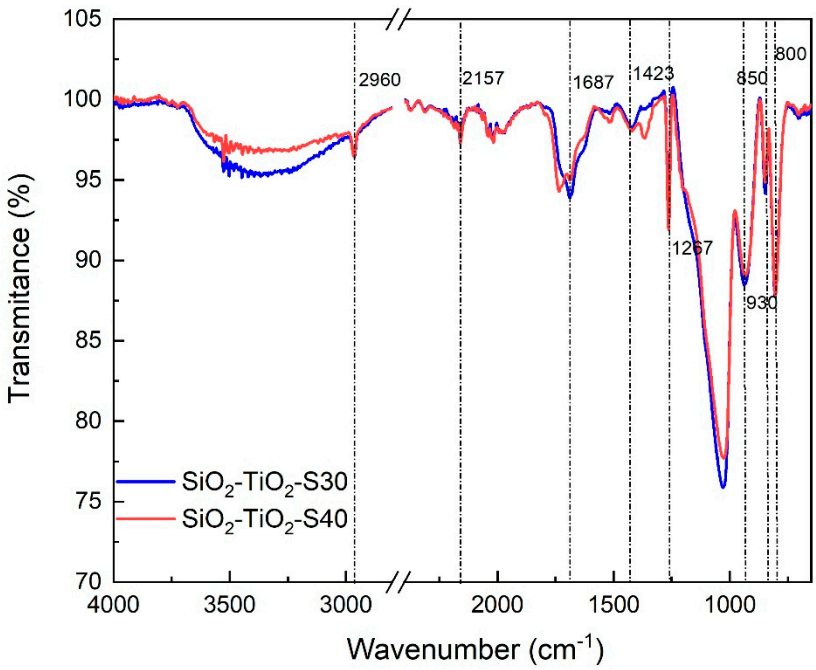

Figure 3. ATR-FTIR spectra of the SiO_2-TiO_2-S30 and S40 composites in the region between 4000 and 650 cm^{-1}.

According to the ATR-FTIR results, it is possible to observe that the chemical changes between the SiO_2-TiO_2 composites are minimal. However, there are significant differences compared to a direct method of sonochemistry application in the synthesis process, as previously reported by Rosales et al. (2022) [24]. These differences have an impact on the properties of the SiO_2-TiO_2 film. The bands of Si-O-Si, SiO_2-O-CH_3 (1200–1000 cm^{-1}) are more intense and broader, indicating an increase in the presence of vibrations of SiO_2 [43]. Furthermore, vibrations 2157 and 1667 cm^{-1} are more intense, attributed to the high availability of Si-H and oxalic acid bonds.

Figure 4 shows the XRD pattern of the SiO_2-TiO_2 film. The diffractogram exhibits the characteristic signal at 25–30° of the SiO_2 amorphous phase (JCPDS PDF No. 46-1045) [44]. In the S30 film, the amorphous of the film is notable, with the signal below 20° being more intense [45]. Additionally, it is possible to observe the characteristic (1 1 0) plane at 27.5° of the TiO_2 rutile phase (JCPDS PDF 21-1276) [46], and (1 0 1) plane at 25.28° of the TiO_2 anatase phase (JCPDS PDF 21-1272), the last one is possible to see only in an S40 film.

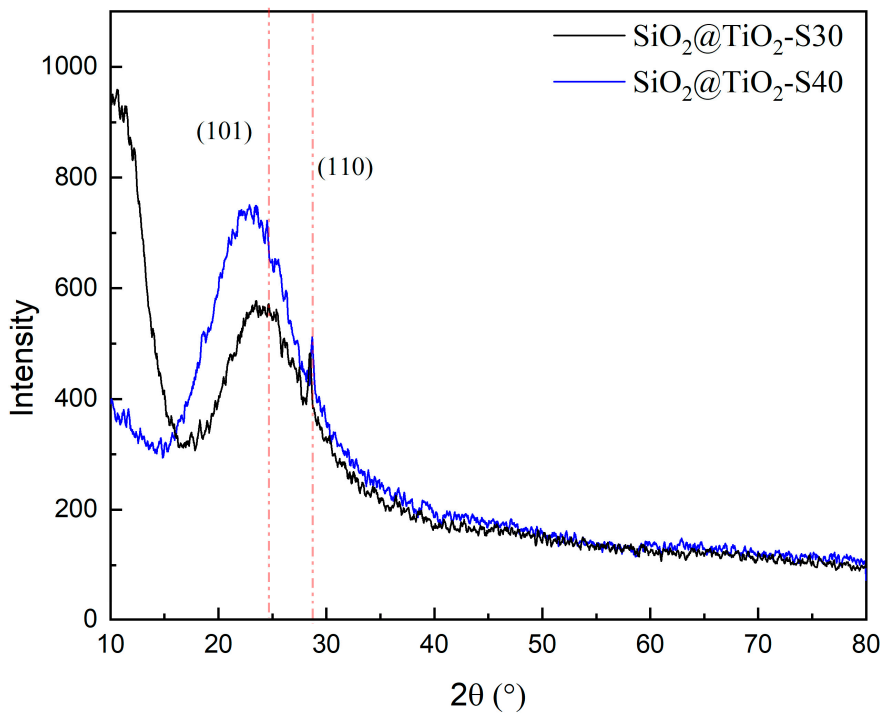

Figure 4. X-ray diffraction patterns of SiO_2-TiO_2-S30 and S40 composites.

The contact angle was determined over aluminum foil and glass substrates to compare the behavior of the SiO_2-TiO_2 films in smooth-rigid and smooth-flexible surfaces, with a contact angle before the application of SiO_2-TiO_2 films of 45 ± 0.3° for glass and 65° for aluminum foil. The SiO_2-TiO_2-S40 film exhibits a contact angle of 92.03° ± 1.48° and 98.45° ± 1.56° (Figure S1) for the aluminum foil and glass substrate, respectively. On the other hand, the SiO_2-TiO_2-S30 film shows a contact angle of 85.3° ± 1.60° and 97.36° ± 1.15° for aluminum foil and glass, respectively (Table S2). The difference between the films S30 and S40 on glass is attributed to the ultrasonication time, corroborating the effect of the sonochemistry in the SiO_2-TiO_2 composite as A. Rosales et al. 2021 reported [24]. In this way, the difference in the contact angles across different surfaces is attributed to (i) the substrate nature, (ii) the method of ultrasonication during the synthesis process, and (iii) the film application technique, which all combined, leads to the formation of cracks over the surface. These micro-fissures help the films' hydrophobic state by facilitating the trapping of air molecules. These micro-fissures can be attributed to the malleability of aluminum foil and the tiny air pockets that can be trapped in the surface [47], resulting in a reduction of around 5 degrees in the contact angle compared to the glass substrate. Despite the decrease in the contact angle according to the surface change, it can be said that the SiO_2-TiO_2 films preserve the hydrophobic properties.

3.2. Antimicrobial Activity Evaluation

The antibacterial activity of SiO_2-TiO_2-S30 and -S40 films was observed against Gram-positive and Gram-negative microorganisms. Figure 5 shows the number of bacteria *E. coli and S. aureus* in terms of CFU after 24 h incubation time. After incubation, the reduction percentage in *E. coli* viable cells was 7.4% and 94.2% for the S30 and S40 films, respectively (Figure 5a). On the other hand, the reduction percentage in viable cells of *S. aureus* was 3.1% and 52.3% for the S30 and S40 films, respectively (Figure 5b). The effect of the SiO_2-TiO_2 films on *S. aureus* was minor than for *E. coli* (see Table S3). The difference in the results is related to the difference between Gram-negative and Gram-positive bacteria, precisely due to the different cell wall structures contained in each bacteria type. A layer of

lipopolysaccharides in *E. coli* shows an affinity for adhering the film to the cell membrane. This layer is lacking in Gram-positive bacteria, leading to resistance [48].

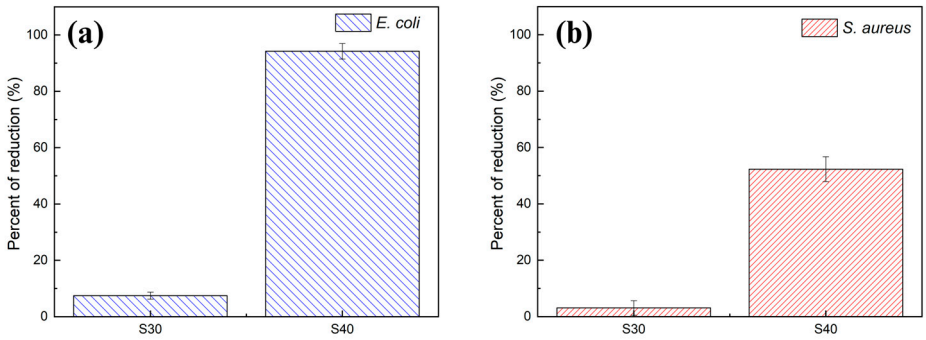

Figure 5. (**a**) *E. coli* and (**b**) *S. aureus* reduction percentages observed after the SiO_2-TiO_2-S30 and S40 treatments.

These results show a significant difference between the SiO_2-TiO_2 films. The SiO_2-TiO_2-S30 exhibits a similar performance compared to the control. Meanwhile, the SiO_2-TiO_2-S40 shows a significative difference compared to the control, proving an inhibition growth of Gram-negative and Gram-positive bacteria, which is more noticeable for the Gram-negative microorganism (*E. coli*). The observed results suggest that the sonochemical reaction time enhances the antibacterial activity by modifying the physicochemical properties, including crystallinity, roughness, and morphological differences, thus increasing antibacterial properties [49]. According to XRD analysis, prolonged sonochemical time (S40) increases the crystallinity of TiO_2, thereby enhancing its antimicrobial properties. Moreover, SiO_2-TiO_2-S40 films exhibit a higher roughness value (18.7 $\pm$ 2.47 nm) compared to SiO_2-TiO_2-S30 (11.55 $\pm$ 1.33 nm) [50] enhancing their hydrophobic properties. It is worth noting that the cell wall composition of Gram-negative bacteria is more highly hydrophobic than the Gram-positive bacteria cell wall [51]. In this context, the coating SiO_2-TiO_2-S40 exhibits significant antibacterial activity against Gram-negative bacteria such as *E. coli* compared to *S. aureus*.

The SiO_2-TiO_2-S40 films were evaluated against two Gram-negative *P. aeruginosa* strain bacteria to confirm the antibacterial action. In this case, it is worth mentioning that a strain resistant to ciprofloxacin was included as it is important to develop new technologies to avoid infections produced by antibiotic-resistant bacteria. The results obtained against both strains of *P. aeruginosa* are shown in Figure 6. After the 24 h incubation period, the reduction percentage in *P. aeruginosa ciprofloxacin-resistant* strain viable cells was 77.8%. Meanwhile, the reduction percentage in *P. aeruginosa* ATCC9072 was 80%, (Table S3).

Vladkova et al. (2020) evaluate the antibacterial activity of TiO_2-SiO_2 with and without Ag NPs using *E. coli* as Gram-negative bacteria, observing damage in the cells by the antimicrobial action of TiO_2-SiO_2 material, with a reduction of 87% in cell viability at 24 h [52]. Yinfan et al. (2019) demonstrated the inactivation of *E. coli* in TiO_2@SiO_2 composites, which improve with the increase in TiO_2 under UVA and visible light irradiation [53].

In this way, the SiO_2-TiO_2-S30 and -S40 films over aluminum foil have antibacterial properties over Gram-positive (*S. aureus*) and Gram-negative (*E. coli*) microorganisms. The films presented significative differences in performance, specifically with the Gram-negative organisms, with a growth reduction percentage up to 80%, as observed in Figure 6 under visible light. Furthermore, it can be proposed that these results are attributed to the hydrophobic and antimicrobial properties of the composite SiO_2-TiO_2, where the increase in the contact angle inhibits the adhesion of microorganisms, consequently inhibiting their growth. Additionally, the presence of the anatase and rutile phase of TiO_2 contributes to the antimicrobial activity. Moreover, the molar ratio of TiO_2 is lower than that of SiO_2, resulting in the combined antimicrobial effect of TiO_2 and the hydrophobic properties of SiO_2 and

PDMS [54]. These differences between SiO_2-TiO_2 films were modified using the indirect method of ultrasound irradiation application and the reaction time of the synthesis method.

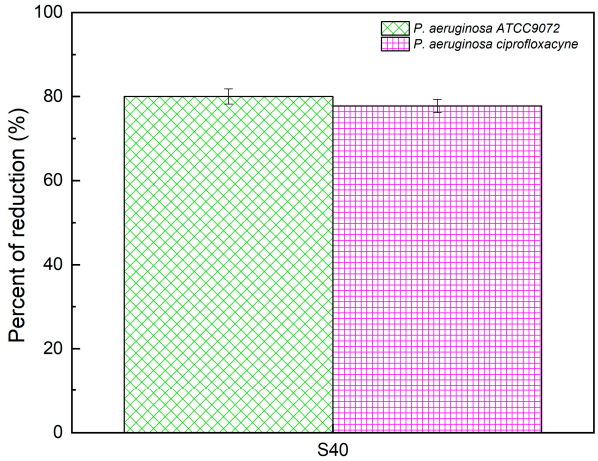

Figure 6. Reduction percentages of *P. aeruginosa ciprofloxacin*-resistant and *P. aeruginosa* (ATCC 9027) after the SiO_2-TiO_2-S40 film treatments.

The effect of SiO_2-TiO_2-S30 and SiO_2-TiO_2-S40 materials observed in *Pseudomonas* strains highlights the importance of developing new materials to counteract the resistance-to-antibiotics problem. In *Pseudomonas* microorganisms, several resistance mechanisms are well-documented, either intrinsic or acquired by horizontal gene transfer [55,56]. Recently, it was demonstrated that in *P. aeruginosa,* resistance to levofloxacin (LVX) is related to its capacity to upregulate DNA repair genes. Also, specific proteomics changes were detected in *P. aeruginosa* as an adaptive response to treatment with several antibiotics [57,58]. Using a SiO_2-TiO_2 composite as coatings is a viable and sustainable alternative to combat these resistant microorganisms. Also, it is worth mentioning that the sonochemical process in the synthesis method allows a material with hydrophobic, mechanical, photocatalytic, and microbial properties to be obtained. Nevertheless, the direct and indirect sonochemistry processes modify the reaction time and temperature due to the energy transfer mechanism, which affects the energy efficiency related to the complete synthesis method but not the final result in the SiO_2-TiO_2 composite [59]. It is essential to clarify that the SiO_2-TiO_2 film is proposed for packaging without direct contact with the food for the alimentary industry. This SiO_2-TiO_2 composite is a suitable option in this research area, related to the previously studied hydrophobic, photocatalytic, and mechanical properties [24,25,60,61].

4. Conclusions

The SiO_2-TiO_2 composite has been previously studied as a hydrophobic and self-cleaning coating with applications over mortar and glass [20,21]. Regarding those results, in this work, the composite was proposed to be studied as a functional SiO_2-TiO_2 film with antimicrobial activity for the alimentary packaging industry, synthesized by the sol–gel method coupled with an indirect ultrasonic method, as is the ultrasonic bath. The SiO_2-TiO_2-S30 and SiO_2-TiO_2-S40 films inhibited cell growth in aluminum foil surfaces. The increase in the sonochemistry reaction time in the synthesis method reflects a change in the hydrophobic and antibacterial activity to establish a morphological relationship between physic-chemical results and antimicrobial performance. The SiO_2-TiO_2-S40 significantly reduced the growth percentage in *E. coli* (94.2%), *P. putida* (80.0%), and *P. aeruginosa* (77.8%) compared to the control. According to the obtained results, the SiO_2-TiO_2-S40 film might be considered a functional film that would help to preserve the safety and increase the shelf-life of foods for innovative packaging in the alimentary industry. The indirect sonication method is effective in developing hydrophobic and antimicrobial surfaces. Previous

research, in our group, tested the physical and chemical durability of the SiO_2-TiO_2 films, obtaining results for up to three months under weathering conditions.

The low intensity of the ultrasonic bath allows obtaining similar results and properties as the direct ultrasonic method. It is important to emphasize that the energy efficiency and the rate of the chemical reaction are lower than with the sonochemical direct method. Nevertheless, in this case, for the SiO_2-TiO_2 composite, it is possible to obtain promising results similar to the same composite synthesized by the sonochemical direct method (self-cleaning, hydrophobicity, microbial, and mechanical properties), which leads to reduced cost production by the instrument's availability.

Supplementary Materials: The following supporting information can be downloaded at: https://www.mdpi.com/article/10.3390/jcs8030104/s1, Table S1: Summarizing information of hydrophobic antimicrobial films; Table S2: Contact angle measurements over glass and aluminum foil; Figure S1: Comparison between glass uncoated and glass coated with SiO_2-TiO_2-S30 and S40 films; Table S3: Images of the bacterial cultures without SiO_2-TiO_2 film (control) and SiO_2-TiO_2-S30 and S40. Refs. [62–68] are cited in Supplementary Materials.

Author Contributions: Conceptualization: K.E. and A.R.; data curation: A.R., H.M. and J.A.C.-C.; formal analysis: A.R., K.E., H.M. and J.A.C.-C.; funding acquisition: K.E.; investigation: A.R., K.E., H.M. and J.A.C.-C.; methodology: A.R. and H.M.; project administration: K.E.; resources: K.E. and J.A.C.-C.; Supervision: K.E. and J.A.C.-C.; validation: J.A.C.-C. and K.E.; roles/writing—original draft: A.R.; writing—review and editing: K.E. and J.A.C.-C. All authors have read and agreed to the published version of the manuscript.

Funding: This research was funded by Universidad Autónoma de Querétaro (FIN202116; FIN202106).

Data Availability Statement: Data can be requested from the corresponding author (Karen Esquivel) if needed.

Acknowledgments: A. Rosales thanks CONACyT for the scholarship granted. K. Esquivel thanks the engineering faculty at UAQ for the financial support given through the Attention to National Problems fund FI-UAQ FIN202116 and the Universidad Autónoma de Querétaro through the fund FONDEC-UAQ 2021FIN202106.

Conflicts of Interest: The authors declare no conflicts of interest.

References

1. Perumal, A.B.; Huang, L.; Nambiar, R.B.; He, Y.; Li, X.; Sellamuthu, P.S. Application of Essential Oils in Packaging Films for the Preservation of Fruits and Vegetables: A Review. *Food Chem.* **2022**, *375*, 131810. [CrossRef] [PubMed]
2. Gupta, V.; Biswas, D.; Roy, S. A Comprehensive Review of Biodegradable Polymer-Based Films and Coatings and Their Food Packaging Applications. *Materials* **2022**, *15*, 5899. [CrossRef]
3. Baghi, F.; Gharsallaoui, A.; Dumas, E.; Ghnimi, S. Advancements in Biodegradable Active Films for Food Packaging: Effects of Nano/Microcapsule Incorporation. *Foods* **2022**, *11*, 760. [CrossRef]
4. Azevedo, A.G.; Barros, C.; Miranda, S.; Machado, A.V.; Castro, O.; Silva, B.; Saraiva, M.; Silva, A.S.; Pastrana, L.; Carneiro, O.S.; et al. Active Flexible Films for Food Packaging: A Review. *Polymers* **2022**, *14*, 2442. [CrossRef]
5. Tiwari, A. *Handbook of Antimicrobial Coatings*; Elsevier: Amsterdam, The Netherlands, 2017; ISBN 978-0-12-811983-9.
6. Sebastian, D.; Yao, C.-W.; Lian, I. Mechanical Durability of Engineered Superhydrophobic Surfaces for Anti-Corrosion. *Coatings* **2018**, *8*, 162. [CrossRef]
7. Gong, X.; He, S. Highly Durable Superhydrophobic Polydimethylsiloxane/Silica Nanocomposite Surfaces with Good Self-Cleaning Ability. *ACS Omega* **2020**, *5*, 4100–4108. [CrossRef] [PubMed]
8. Das, A.; Dhar, M.; Manna, U. Small Molecules Derived Tailored-Superhydrophobicity on Fibrous and Porous Substrates—With Superior Tolerance. *Chem. Eng. J.* **2022**, *430*, 132597. [CrossRef]
9. Vasile, C. Polymeric Nanocomposites and Nanocoatings for Food Packaging: A Review. *Materials* **2018**, *11*, 1834. [CrossRef]
10. Ogunsona, E.O.; Muthuraj, R.; Ojogbo, E.; Valerio, O.; Mekonnen, T.H. Engineered Nanomaterials for Antimicrobial Applications: A Review. *Appl. Mater. Today* **2020**, *18*, 100473. [CrossRef]
11. Aguirre-Joya, J.A.; De Leon-Zapata, M.A.; Alvarez-Perez, O.B.; Torres-León, C.; Nieto-Oropeza, D.E.; Ventura-Sobrevilla, J.M.; Aguilar, M.A.; Ruelas-Chacón, X.; Rojas, R.; Ramos-Aguiñaga, M.E.; et al. Chapter 1—Basic and Applied Concepts of Edible Packaging for Foods. In *Food Packaging and Preservation*; Grumezescu, A.M., Holban, A.M., Eds.; Handbook of Food Bioengineering; Academic Press: Cambridge, MA, USA, 2018; pp. 1–61, ISBN 978-0-12-811516-9.

12. Sharma, R.; Jafari, S.M.; Sharma, S. Antimicrobial Bio-Nanocomposites and Their Potential Applications in Food Packaging. *Food Control* **2020**, *112*, 107086. [CrossRef]
13. Ferreira, T.P.M.; Nepomuceno, N.C.; Medeiros, E.L.G.; Medeiros, E.S.; Sampaio, F.C.; Oliveira, J.E.; Oliveira, M.P.; Galvão, L.S.; Bulhões, E.O.; Santos, A.S.F. Antimicrobial Coatings Based on Poly(Dimethyl Siloxane) and Silver Nanoparticles by Solution Blow Spraying. *Prog. Org. Coat.* **2019**, *133*, 19–26. [CrossRef]
14. Shome, A.; Das, A.; Borbora, A.; Dhar, M.; Manna, U. Role of Chemistry in Bio-Inspired Liquid Wettability. *Chem. Soc. Rev.* **2022**, *51*, 5452–5497. [CrossRef]
15. Verma, J.; Gupta, A.; Kumar, D. Steel Protection by SiO_2/TiO_2 Core-Shell Based Hybrid Nanocoating. *Prog. Org. Coat.* **2022**, *163*, 106661. [CrossRef]
16. Trajkovska Petkoska, A.; Daniloski, D.; D'Cunha, N.M.; Naumovski, N.; Broach, A.T. Edible Packaging: Sustainable Solutions and Novel Trends in Food Packaging. *Food Res. Int.* **2021**, *140*, 109981. [CrossRef]
17. Dash, K.K.; Deka, P.; Bangar, S.P.; Chaudhary, V.; Trif, M.; Rusu, A. Applications of Inorganic Nanoparticles in Food Packaging: A Comprehensive Review. *Polymers* **2022**, *14*, 521. [CrossRef]
18. Tzhayik, O.; Lipovsky, A.; Gedanken, A. Sonochemical Fabrication of Edible Fragrant Antimicrobial Nano Coating on Textiles and Polypropylene Cups. *Ultrason. Sonochem.* **2017**, *38*, 614–621. [CrossRef]
19. Qin, Y.; Xue, L.; Hu, Y.; Qiu, C.; Jin, Z.; Xu, X.; Wang, J. Green Fabrication and Characterization of Debranched Starch Nanoparticles via Ultrasonication Combined with Recrystallization. *Ultrason. Sonochem.* **2020**, *66*, 105074. [CrossRef]
20. Asgharzadehahmadi, S.; Abdul Raman, A.A.; Parthasarathy, R.; Sajjadi, B. Sonochemical Reactors: Review on Features, Advantages and Limitations. *Renew. Sustain. Energy Rev.* **2016**, *63*, 302–314. [CrossRef]
21. Mallakpour, S.; Azadi, E. Chapter 11—Sonochemical Protocol for the Organo-Synthesis of TiO_2 and Its Hybrids: Properties and Applications. In *Green Sustainable Process for Chemical and Environmental Engineering and Science*; Inamuddin Boddula, R., Asiri, A.M., Eds.; Elsevier: Amsterdam, The Netherlands, 2020; pp. 287–323, ISBN 978-0-12-819540-6.
22. Schneider, T.; Westermann, M.; Glei, M. Impact of Ultrasonication on the Delivered Dose of Metal Oxide Particle Dispersions In Vitro. *Colloids Surf. A Physicochem. Eng. Asp.* **2020**, *601*, 125026. [CrossRef]
23. Priego-Capote, F.; Luque de Castro, M.D. Analytical Uses of Ultrasound I. Sample Preparation. *TrAC Trends Anal. Chem.* **2004**, *23*, 644–653. [CrossRef]
24. Rosales, A.; Ortiz-Frade, L.; Medina-Ramirez, I.E.; Godínez, L.A.; Esquivel, K. Self-Cleaning of SiO_2-TiO_2 Coating: Effect of Sonochemical Synthetic Parameters on the Morphological, Mechanical, and Photocatalytic Properties of the Films. *Ultrason. Sonochem.* **2021**, *73*, 105483. [CrossRef]
25. Rosales, A.; Maury-Ramírez, A.; Gutiérrez, R.M.-D.; Guzmán, C.; Esquivel, K. SiO_2@TiO_2 Coating: Synthesis, Physical Characterization and Photocatalytic Evaluation. *Coatings* **2018**, *8*, 120. [CrossRef]
26. Margoy, D.; Gouzman, I.; Grossman, E.; Bolker, A.; Eliaz, N.; Verker, R. Epoxy-Based Shape Memory Composite for Space Applications. *Acta Astronaut.* **2021**, *178*, 908–919. [CrossRef]
27. Kapridaki, C.; Pinho, L.; Mosquera, M.J.; Maravelaki-Kalaitzaki, P. Producing Photoactive, Transparent and Hydrophobic SiO_2-Crystalline TiO_2 Nanocomposites at Ambient Conditions with Application as Self-Cleaning Coatings. *Appl. Catal. B Environ.* **2014**, *156–157*, 416–427. [CrossRef]
28. Kapridaki, C.; Verganelaki, A.; Dimitriadou, P.; Maravelaki-Kalaitzaki, P. Conservation of Monuments by a Three-Layered Compatible Treatment of TEOS-Nano-Calcium Oxalate Consolidant and TEOS-PDMS-TiO_2 Hydrophobic/Photoactive Hybrid Nanomaterials. *Materials* **2018**, *11*, 684. [CrossRef]
29. Xiang, B.; Zhang, J. Using Ultrasound-Assisted Dispersion and In Situ Emulsion Polymerization to Synthesize TiO_2/ASA (Acrylonitrile-Styrene-Acrylate) Nanocomposites. *Compos. Part B Eng.* **2016**, *99*, 196–202. [CrossRef]
30. Sharifalhoseini, Z.; Entezari, M.H.; Jalal, R. Direct and Indirect Sonication Affect Differently the Microstructure and the Morphology of ZnO Nanoparticles: Optical Behavior and Its Antibacterial Activity. *Ultrason. Sonochem.* **2015**, *27*, 466–473. [CrossRef]
31. Rivero, P.J.; Maeztu, J.D.; Berlanga, C.; Miguel, A.; Palacio, J.F.; Rodriguez, R. Hydrophobic and Corrosion Behavior of Sol-Gel Hybrid Coatings Based on the Combination of TiO_2 NPs and Fluorinated Chains for Aluminum Alloys Protection. *Metals* **2018**, *8*, 1076. [CrossRef]
32. Salehi, M.; Mozammel, M.; Emarati, S.M.; Alinezhadfar, M. The Role of TiO_2 Nanoparticles on the Topography and Hydrophobicity of Electrodeposited Ni-TiO_2 Composite Coating. *Surf. Topogr. Metrol. Prop.* **2020**, *8*, 025008. [CrossRef]
33. Widati, A.A.; Nuryono, N.; Kartini, I. Water-Repellent Glass Coated with SiO_2-TiO_2-Methyltrimethoxysilane through Sol-Gel Coating. *AIMS Mater. Sci.* **2019**, *6*, 10–24. [CrossRef]
34. Sebastian, D.; Yao, C.-W.; Lian, I. Abrasion Resistance of Superhydrophobic Coatings on Aluminum Using PDMS/SiO_2. *Coatings* **2018**, *8*, 414. [CrossRef]
35. Ruggiero, L.; Fidanza, M.R.; Iorio, M.; Tortora, L.; Caneva, G.; Ricci, M.A.; Sodo, A. Synthesis and Characterization of TEOS Coating Added with Innovative Antifouling Silica Nanocontainers and TiO_2 Nanoparticles. *Front. Mater.* **2020**, *7*, 185. [CrossRef]
36. Shao, L.; Liu, H.; Zeng, W.; Zhou, C.; Li, D.; Wang, L.; Lan, Y.; Xu, F.; Liu, G. Immobilized and Photocatalytic Performances of PDMS-SiO_2-chitosan@TiO_2 Composites on Pumice under Simulated Sunlight Irradiation. *Appl. Surf. Sci.* **2019**, *478*, 1017–1026. [CrossRef]
37. Xie, J.; Hu, J.; Lin, X.; Fang, L.; Wu, F.; Liao, X.; Luo, H.; Shi, L. Robust and Anti-Corrosive PDMS/SiO_2 Superhydrophobic Coatings Fabricated on Magnesium Alloys with Different-Sized SiO_2 Nanoparticles. *Appl. Surf. Sci.* **2018**, *457*, 870–880. [CrossRef]

38. González-Rivera, J.; Iglio, R.; Barillaro, G.; Duce, C.; Tinè, M.R. Structural and Thermoanalytical Characterization of 3D Porous PDMS Foam Materials: The Effect of Impurities Derived from a Sugar Templating Process. *Polymers* **2018**, *10*, 616. [CrossRef]
39. Orcel, G.; Phalippou, J.; Hench, L.L. Structural Changes of Silica Xerogels during Low Temperature Dehydration. *J. Non-Cryst. Solids* **1986**, *88*, 114–130. [CrossRef]
40. Zhu, Z.; Wang, Z.; Zhou, Y.; Wei, Y.; She, A. Synthesis and Structure of Calcium Silicate Hydrate (C-S-H) Modified by Hydroxyl-Terminated Polydimethylsiloxane (PDMS). *Constr. Build. Mater.* **2021**, *267*, 120731. [CrossRef]
41. Wang, P.; Chen, M.; Han, H.; Fan, X.; Liu, Q.; Wang, J. Transparent and Abrasion-Resistant Superhydrophobic Coating with Robust Self-Cleaning Function in Either Air or Oil. *J. Mater. Chem. A* **2016**, *4*, 7869–7874. [CrossRef]
42. Primeau, N.; Vautey, C.; Langlet, M. The Effect of Thermal Annealing on Aerosol-Gel Deposited SiO2 Films: A FTIR Deconvolution Study. *Thin Solid Films* **1997**, *310*, 47–56. [CrossRef]
43. Royon, M.; Vocanson, F.; Jamon, D.; Royer, F.; Marin, E.; Morana, A.; Campanella, C.; Boukenter, A.; Ouerdane, Y.; Jourlin, Y.; et al. Impact of γ-Rays Irradiation on Hybrid TiO_2-SiO_2 Sol-Gel Films Doped with RHODAMINE 6G. *Materials* **2021**, *14*, 5754. [CrossRef]
44. Xue, S.-H.; Xie, H.; Ping, H.; Li, Q.-C.; Su, B.-L.; Fu, Z.-Y. Induced Transformation of Amorphous Silica to Cristobalite on Bacterial Surfaces. *RSC Adv.* **2015**, *5*, 71844–71848. [CrossRef]
45. Tsukimura, K.; Miyoshi, Y.; Takagi, T.; Suzuki, M.; Wada, S. Amorphous Nanoparticles in Clays, Soils and Marine Sediments Analyzed with a Small Angle X-ray Scattering (SAXS) Method. *Sci. Rep.* **2021**, *11*, 6997. [CrossRef] [PubMed]
46. Scarpelli, F.; Mastropietro, T.F.; Poerio, T.; Godbert, N. *Mesoporous TiO_2 Thin Films: State of the Art*; IntechOpen: London, UK, 2018; ISBN 978-1-78923-327-8.
47. Jadhavar, S.B.; Sutar, R.S.; Latthe, S.S.; Vhatkar, R.S. Preparation of Superhydrophobic Coating Using Silica–PMMA Nanocomposite. *Macromol. Symp.* **2020**, *393*, 2000161. [CrossRef]
48. Hajizadeh, H.; Peighambardoust, S.J.; Peighambardoust, S.H.; Peressini, D. Physical, Mechanical, and Antibacterial Characteristics of Bio-Nanocomposite Films Loaded with Ag-Modified SiO_2 and TiO_2 Nanoparticles. *J. Food Sci.* **2020**, *85*, 1193–1202. [CrossRef] [PubMed]
49. Jagadeeshan, S.; Parsanathan, R. Nano-Metal Oxides for Antibacterial Activity. In *Advanced Nanostructured Materials for Environmental Remediation*; Naushad, M., Rajendran, S., Gracia, F., Eds.; Environmental Chemistry for a Sustainable World; Springer International Publishing: Cham, Switzerland, 2019; pp. 59–90, ISBN 978-3-030-04477-0.
50. Pirsa, S.; Farshchi, E.; Roufegarinejad, L. Antioxidant/Antimicrobial Film Based on Carboxymethyl Cellulose/Gelatin/TiO_2–Ag Nano-Composite. *J. Polym. Environ.* **2020**, *28*, 3154–3163. [CrossRef]
51. Wiener, M.C.; Horanyi, P.S. How Hydrophobic Molecules Traverse the Outer Membranes of Gram-Negative Bacteria. *Proc. Natl. Acad. Sci. USA* **2011**, *108*, 10929–10930. [CrossRef] [PubMed]
52. Vladkova, T.; Angelov, O.; Stoyanova, D.; Gospodinova, D.; Gomes, L.; Soares, A.; Mergulhao, F.; Ivanova, I. Magnetron Co-Sputtered TiO_2/SiO_2/Ag Nanocomposite Thin Coatings Inhibiting Bacterial Adhesion and Biofilm Formation. *Surf. Coat. Technol.* **2020**, *384*, 125322. [CrossRef]
53. Chen, Y.; Tang, X.; Gao, X.; Zhang, B.; Luo, Y.; Yao, X. Antimicrobial Property and Photocatalytic Antibacterial Mechanism of the TiO_2-Doped SiO_2 Hybrid Materials under Ultraviolet-Light Irradiation and Visible-Light Irradiation. *Ceram. Int.* **2019**, *45*, 15505–15513. [CrossRef]
54. Kapridaki, C.; Maravelaki-Kalaitzaki, P. TiO_2–SiO_2–PDMS Nano-Composite Hydrophobic Coating with Self-Cleaning Properties for Marble Protection. *Prog. Org. Coat.* **2013**, *76*, 400–410. [CrossRef]
55. Pachori, P.; Gothalwal, R.; Gandhi, P. Emergence of Antibiotic Resistance Pseudomonas Aeruginosa in Intensive Care Unit; a Critical Review. *Genes Dis.* **2019**, *6*, 109–119. [CrossRef]
56. Rocha, A.J.; de Oliveira Barsottini, M.R.; Rocha, R.R.; Laurindo, M.V.; de Moraes, F.L.L.; da Rocha, S.L. *Pseudomonas Aeruginosa*: Virulence Factors and Antibiotic Resistance Genes. *Braz. Arch. Biol. Technol.* **2019**, *62*, e19180503. [CrossRef]
57. Wüllner, D.; Gesper, M.; Haupt, A.; Liang, X.; Zhou, P.; Dietze, P.; Narberhaus, F.; Bandow, J.E. Adaptive Responses of Pseudomonas Aeruginosa to Treatment with Antibiotics. *Antimicrob. Agents Chemother.* **2022**, *66*, e00878-21. [CrossRef] [PubMed]
58. Li, F.-F.; Zhao, W.-H.; Tangadanchu, V.K.R.; Meng, J.-P.; Zhou, C.-H. Discovery of Novel Phenylhydrazone-Based Oxindole-Thiolazoles as Potent Antibacterial Agents toward Pseudomonas Aeruginosa. *Eur. J. Med. Chem.* **2022**, *239*, 114521. [CrossRef] [PubMed]
59. Kimura, T.; Sakamoto, T.; Leveque, J.-M.; Sohmiya, H.; Fujita, M.; Ikeda, S.; Ando, T. Standardization of Ultrasonic Power for Sonochemical Reaction. *Ultrason. Sonochem.* **1996**, *3*, S157–S161. [CrossRef]
60. Deon, M.; Carminatti Ricardi, N.; Carvalho de Andrade, R.; Hertz, P.F.; Nicolodi, S.; Costa, T.M.H.; Bussamara, R.; Benvenutti, E.V.; de Menezes, E.W. Designing a Support for Lipase Immobilization Based on Magnetic, Hydrophobic, and Mesoporous Silica. *Langmuir* **2020**, *36*, 10147–10155. [CrossRef]
61. Santiago, A.A.G.; Gondim, J.G.S.; Tranquilin, R.L.; Silva, F.S.; Fernandez, F.F.; Costa, M.C.B.; Motta, F.V.; Bomio, M.R.D. Development of ZnO/PDMS Nanocomposite with Photocatalytic/Hydrophobic Multifunction. *Chem. Phys. Lett.* **2020**, *740*, 137051. [CrossRef]
62. Atefyekta, S.; Ercan, B.; Karlsson, J.; Taylor, E.; Chung, S.; Webster, T.J.; Andersson, M. Antimicrobial Performance of Mesoporous Titania Thin Films: Role of Pore Size, Hydrophobicity, and Antibiotic Release. *Int. J. Nanomed.* **2016**, *11*, 977–990. [CrossRef]

63. Ni, S.; Zhang, H.; Dai, H.; Xiao, H. Starch-Based Flexible Coating for Food Packaging Paper with Exceptional Hydrophobicity and Antimicrobial Activity. *Polymers* **2018**, *10*, 1260. [CrossRef] [PubMed]
64. Bordenave, N.; Grelier, S.; Coma, V. Hydrophobization and Antimicrobial Activity of Chitosan and Paper-Based Packaging Material. *Biomacromolecules* **2010**, *11*, 88–96. [CrossRef] [PubMed]
65. Wang, B.; Liu, H.; Wang, Z.; Shi, S.; Nan, K.; Xu, Q.; Ye, Z.; Chen, H. Retracted Article: A Self-Defensive Antibacterial Coating Acting through the Bacteria-Triggered Release of a Hydrophobic Antibiotic from Layer-by-Layer Films. *J. Mater. Chem. B* **2017**, *5*, 1498–1506. [CrossRef] [PubMed]
66. Lin, X.; Li, S.; Jung, J.; Ma, W.; Li, L.; Ren, X.; Sun, Y.; Huang, T.-S. PHB/PCL Fibrous Membranes Modified with SiO_2@TiO_2-Based Core@shell Composite Nanoparticles for Hydrophobic and Antibacterial Applications. *RSC Adv.* **2019**, *9*, 23071–23080. [CrossRef] [PubMed]
67. Shahnooshi, M.; Eshaghi, A.; Aghaei, A.A. Transparent Anti-Fogging and Anti-Scratch SiO_2/SiO_2–TiO_2 Thin Film on Polycarbonate Substrate. *Mater. Res. Express* **2019**, *6*, 086447. [CrossRef]
68. Sazvar, A.; Alavi, S.M.S.; Sarpoolaky, H. Effect of Chemical Composition on Microstructure and Hydrophobic Properties of SiO_2-TiO_2@PDMS Coating. *Iran. J. Mater. Sci. Eng.* **2023**, *20*, 1–11. [CrossRef]